

# Polyethylene-Montmorillonite Nanocomposites: Preparation, Characterization and Properties

Liqiang Cui, Hyun Yong Cho, Joong-Won Shin, Naresh Hiralal Tarte, Seong Ihl Woo\*

**Summary:** Polyethylene(PE)/clay nanocomposites have been successfully prepared by *in situ* polymerization with an intercalation catalyst titanium-montmorillonite (Ti-MMT) and analyzed by X-ray diffraction analysis (XRD), Fourier transform infrared analysis (FT-IR), Transmission electron microscopy (TEM), differential scanning calorimetry (DSC), thermal gravimetric analysis (TGA) and tensile testing. XRD and TEM indicate that the clay is exfoliated into nanometer size and disorderedly dispersed in the PE matrix, and the PE crystallinity of PE/clay nanocomposite declines to 15~30%. Compared with pure PE, PE/clay nanocomposites behave higher thermal, physical and mechanical properties; the layer structure of the clay decreases the polymerization activity and produce polymer with a high molecular weight. For PE/clay nanocomposites, the highest tensile strength of 33.4 MPa and Young's modulus of 477.4 MPa has been achieved when clay content is 7.7 wt %. The maximum thermal decomposition temperature is up to 110 °C higher, but the thermal decomposition temperature of the PE/clay nanocomposites decreases with the increases of the clay contents in the PE matrix.

**Keywords:** clay; *in situ* polymerization; nanocomposites; polyethylene; property

## Introduction

Polymer-layered silicate nanocomposites are a new class of organic polymer materials, which serve as novel composite materials.<sup>[1]</sup> Clay with a few weight percentage in the reinforced polymer nanocomposites strongly influence polymer macrocomposite properties. Some properties of the polymer, such as higher heat distortion temperatures, an enhanced flame resistance, an increased modulus, better barrier properties, a reduced thermal expansion coefficient, altered electronic and optical properties have been achieved.<sup>[1–4]</sup> After the successful synthesis of nylon-6/clay nanocomposite, an inter-

calation method for synthesizing polymer/clay nanocomposites has received a large amount of attention.<sup>[5]</sup> Both melt intercalation<sup>[6]</sup> and *in situ* polymerization<sup>[7]</sup> methods have been attempted for synthesizing polyolefin/clay nanocomposites; *In situ* polymerization has been proved to be a promising method for preparing fully exfoliated nanocomposites of polyolefin.

Metallocene catalysts supported on the clay have been used to polymerize ethylene, but an excessive amount of cocatalyst methylaluminoxane (MAO) is needed for activation of metallocene catalysts.<sup>[7a]–[7h]</sup> More recently, many Ziegler-Natta catalysts have been employed to prepare polyolefin nanocomposites.<sup>[7i]–[7k]</sup> Rong et al.<sup>[7i]</sup> used Ziegler-Natta catalyst supported on the surface of nanoscale crystal of palygorskite to initiate ethylene polymerization on the surface of the fiber. Yang et al.<sup>[7j]</sup> used MMT/MgCl<sub>2</sub>/TiCl<sub>4</sub>/AlEt<sub>3</sub> catalyst system to synthesize PE nanocomposites. The

Department of Chemical and Biomolecular Engineering (BK21 graduate program) & Center for Ultramicrochemical Process Systems (CUPS), Korea Advanced Institute of Science and Technology, 373-1 Guseong-dong, Yuseong-gu, Daejeon 305-701, Republic of Korea  
Fax: +82-42-869-8890;  
E-mail: siwoo@kaist.ac.kr

nanoscale dispersion of the MMT layer in the PE matrix was characterized. The tensile strength was significantly improved compared to that of pure PE. Kwak et al.<sup>[7k]</sup> reported that  $\text{TiCl}_4$  firstly reacted with the modified montmorillonite (MMT-OH) at 30 °C, and then the cocatalyst  $\text{Et}_3\text{Al}$  was introduced to activate  $\text{TiCl}_4$ . Complete exfoliation of the MMT during Ti-based Ziegler-Natta polymerization has been successfully carried out, but the clay dispersion is not uniform.

In this paper, we present a novel method to synthesize PE/clay nanocomposites by *in situ* polymerization. The state of dispersion of the clay layers in the PE matrix has been investigated. The physical mechanical properties and thermal stability of the PE/clay nanocomposites are also discussed.

## Experimental Part

### Materials

Sodium montmorillonite (Kunipia F, Cation Exchange Capacity (CEC) 119 meq/100 g, surface area: 750 m<sup>2</sup>/g) supplied by Kunimine Co. was used as received. Titanium tetraethoxide and  $\text{Al}(\text{i-Bu})_3$  (from Aldrich Co.) were used without further purification. Decahydronaphthalene (99%) was supplied by Kanto Chemical Co. Toluene (J. T. Baker Chem. Co.) of extra pure grade was purified by refluxing over sodium metal/benzophenone in a nitrogen atmosphere. Polymerization purity grade ethylene, which was donated by Daerim Petroleum Company, was used after passing the oxy trap and molecular sieve trap to remove oxygen and water.

### Immobilization of Catalyst

Intercalation of titanium polyoxocation in the layers of the Kunipia F was prepared according to the literatures.<sup>[8–10]</sup> Typically, the titanium polyoxocation solution was prepared through slow addition of titanium tetraethoxide to the vigorously stirred 5 M HCl solution and consequent reaction for 10 h at room temperature. The molar ratio of HCl to the titanium tetraethoxide was

2:1. After the titanium polyoxocation solution was added to a clay suspension (1 g/L) at room temperature and the mixture was stirred for three hours. The ratio of the Ti to clay was 25 mol:1 equivalent (CEC) of the clay. The precipitate was washed repeatedly with deionized water several times until no chlorine ion was detected with 0.1 N  $\text{AgNO}_3$  solutions. The product (Ti-MMT) was then vacuum-dried and ground into a fine powder. The contents of titanium in Ti-MMT were measured by inductively coupled plasma-atomic emission spectroscopy (ICP-AES).

### Preparation of the PE/Clay Nanocomposites

The ethylene polymerization was carried out in a 1 L Parr reactor. 300 ml toluene, Ti-MMT slurry and  $\text{Al}(\text{i-Bu})_3$  with various molar ratio were introduced into the reactor. The polymerization was started as the ethylene was introduced into the reactor. The polymerization was carried out at 60 °C with supplying ethylene under a pressure of 6.5 atm to keep the polymerization proceeding for a designated period of time. The reaction was terminated by the addition of an acidified ethanol solution. The polymer was precipitated, and then dried under a vacuum at 60 °C for 12 h to obtain the PE/clay nanocomposites.

### Characterization

X-ray diffraction (XRD) was carried out by a Rigaku X-ray diffractometer ( $\text{Cu-K}\alpha$  radiation with  $\lambda = 0.15406$  nm) at room temperature. The diffractograms were scanned in  $2\theta$  ranges from 1.0 to 10 ° at a rate of 1 °/min. Fourier transform infrared (FT-IR) spectra were obtained in the range of 4000 ~ 400  $\text{cm}^{-1}$  at a resolution of 4.0  $\text{cm}^{-1}$  using a MAGNA-IR 560 at room temperature. The KBr pellet method was used in the measurement. A transmission electron microscope (Philips CM20) operated at an acceleration voltage of 120 kV was used to observe the dispersibility of the clay in the hybrids. Ultrathin sections 70 ~ 80 nm in thickness were prepared by an ultramicrotome Leica EM FCS. The

tensile test was carried out according to ASTM D 882 with an Instron 5583. The crosshead speed was set at 10 mm/min. DSC measurement was performed on a TA2000 differential scanning calorimeter at a heating or cooling rate of 10 °C/min in a nitrogen atmosphere in the range of 30 to 200 °C. In order to get rid of the influence of thermal history, two continuous scanning cycles were carried out and the data obtained from the second scanning were accepted. The thermal decomposition temperature was determined by thermogravimetric analysis (TGA) under nitrogen flow protection in a scanning range of 50–700 °C at the rate of 10 °C/min. Viscosity-average molecular weight ( $M_\eta$ ) of the PE nanocomposites was measured using a viscometer at 135 °C with decahydronaphthalene as the solvent according to  $[\eta] = 2.30 \times 10^{-4} M_\eta^{0.82}$ .<sup>[11]</sup>

## Results and Discussion

### Structure and Properties of the Ti-MMT

It is an important step for producing *in situ* polymerized nanocomposites to fix the

catalyst into the silicate layers of the clay. With Na<sup>+</sup>-MMT (Kunipia F) as a supporting medium, the titanium alkoxide was firstly hydrolyzed and titanium polyoxocation ions formed; then cation exchanged reaction was carried out by adding the polyoxocation solution to the clay suspension. Figure 1 shows the XRD patterns of pristine MMT (a) and Ti-MMT (b). The Ti-MMT presents a  $d_{(001)}$  diffraction peak at  $2\theta = 1.5^\circ$  ( $d_{(001)} = 5.86$  nm) resulting from the formation of intercalation and a  $d_{(001)}$  diffraction peak at  $2\theta = 7.5^\circ$  ( $d_{(001)} = 1.19$  nm) corresponding to the pristine MMT. Titanium polyoxocation intercalation of MMT was also reported to achieve relatively large basal spacing ( $d_{(001)} = 2.50$  nm), but the exact composition of the pillaring titanium polyoxocation was not yet known.<sup>[9–10]</sup> Compared with previous reports, Ti-MMT that we obtained has much larger basal spacing. Thus it can be known that the monomer will be more easy to penetrate into the interlayer of the clay and polymerized in it, making layers easily exfoliated by the polymer chain. In our experiment, the much larger intercalating ions have been obtained, confirming the

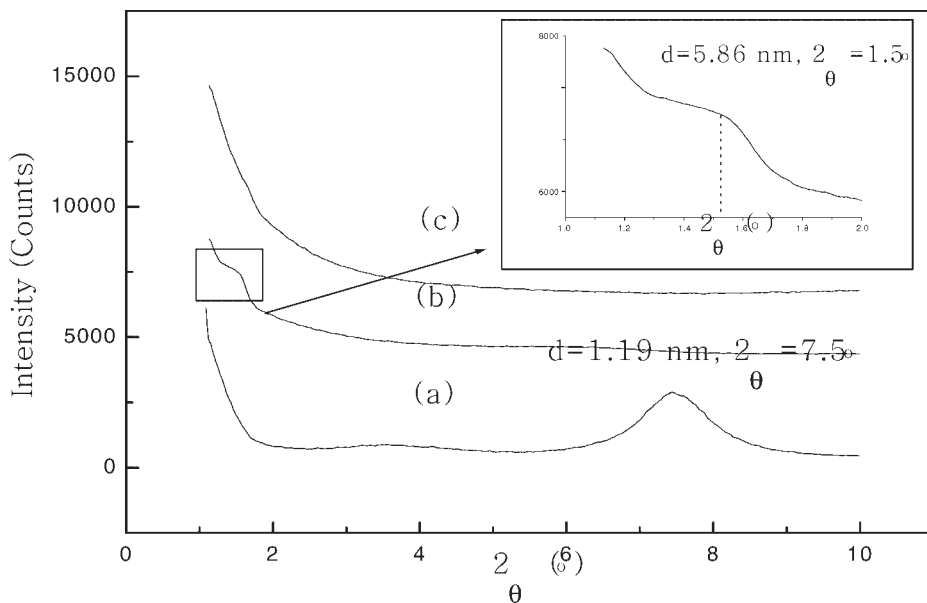


**Figure 1.**

WAXD patterns of (a) pristine MMT (b) Ti-MMT and the PE/clay nanocomposites (c) (from sample PE-1).

big expansion in the interlayer spacing of the clay.

The metal elemental analysis of the pristine MMT and Ti-MMT, shows that the titanium amount increases from 0.08 wt % in pristine MMT to 33.7 wt % in Ti-MMT. The amounts of other cations pronouncedly decrease, such as amount of sodium decreases from 0.89 wt % to 0.0085 wt %. This result indicates that large amounts of cations between layers of MMT have been exchanged by titanium ions.

The Ti-MMT was used to catalyze ethylene polymerization and the results were shown in Table 1. It is possible to control the clay contents in the PE matrix by varying the initial clay loading or polymerization time.<sup>[12]</sup> With the increasing amount of Ti-MMT, the catalytic activity decreases, but the molecular weights of PE/clay nanocomposites are higher than that of pure PE. The low catalytic activity observed in this polymerization should be correlated with the layer structure of the clay. The laminated structure of the silicates restrains the mass transfer of the monomers and make the catalyst easily deactivated. When polymerization is carried out in such a nanoscopic space, the active species can be easily protected from other chemicals, which will cause the termination of the propagation of the polymer chain. In such a situation, polymer with a high molecular weight could be produced when the silicate registry is retained. However, the amounts of intercalated catalyst increase with Ti-MMT

resulting in the decrease of molecular weight of PE/clay nanocomposites from  $7.0 \times 10^5$  to  $3.9 \times 10^5$ . Extraction of polyethylene chains from the PE/clay composites was carried out using reflux decahydronaphthalene in a Soxhlet extractor for 24 h. Polyethylene catalyzed by homogeneous catalyst (from sample PE-0) is totally extracted, but only part of the polyethylene could be extracted and extracted amount of the PE significantly decreases with the increase of the clay contents in the PE matrix. When mixed with the PE, the clay layers will undoubtedly stiffen the PE chains. At the same time, the clay also impeded the movements of the polymer chains, especially when the particular network is formed.<sup>[13]</sup>

The representative FT-IR spectra of the pristine MMT (a), pure PE (b) and a series of extracted PE/clay nanocomposites (c ~ e) are displayed in Figure 2. In the IR spectrum of pristine MMT, characteristic absorbance bands occur in the following assignment: –OH stretching at  $3632\text{ cm}^{-1}$ , coordination and absorbed water peak at  $3430$  and  $1640\text{ cm}^{-1}$ , Si–O stretching at  $1040\text{ cm}^{-1}$  and Al–O stretching at  $550\text{ cm}^{-1}$ .<sup>[7d]</sup> The characteristic vibration bands of the PE are C–H stretching at  $2855$  and  $2950\text{ cm}^{-1}$  and  $1470\text{ cm}^{-1}$  ( $\delta_{\text{C-H}}$ ). In the IR spectrum of the PE/clay composites, the presence of both the characteristic group frequencies of PE and MMT can be found. These results show that only part of the PE can be extracted from the nanocomposites, and the rest of the PE chains stay immobilized inside and/or on the layered sili-

**Table 1.**

Results of ethylene polymerization by *in situ* polymerization with Ti-MMT

Sample	Amount of Ti-MMT (mg)	Activity <sup>a)</sup>	Clay mass fraction (wt %) <sup>b)</sup>	Extracted in decaline (wt %)	$M_n (\times 10^{-5})$
PE-0 <sup>c)</sup>	0	2300	0	100	3.6
PE-1	187.5	450	3.9	65.7	7.0
PE-2	375.0	380	6.8	36.3	5.1
PE-3	562.5	310	7.7	24.1	3.9

Polymerization condition: Al(*i*-Bu)<sub>3</sub> as cocatalyst, [Al]/[Ti]=10; toluene as solvent; polymerization temperature: 60 °C, polymerization time 2 h, ethylene pressure 6.5 atm;

<sup>a)</sup> Activity ( $\text{PE}_g/\text{Ti}_{\text{mol}} \cdot \text{h} \cdot \text{atm}$ );

<sup>b)</sup> Determined by TGA;

<sup>c)</sup> Sample PE-0 synthesized by homogeneous catalyst Ti(OEt)<sub>4</sub>/Al(*i*-Bu)<sub>3</sub>, the other polymerization conditions are same as PE-3.

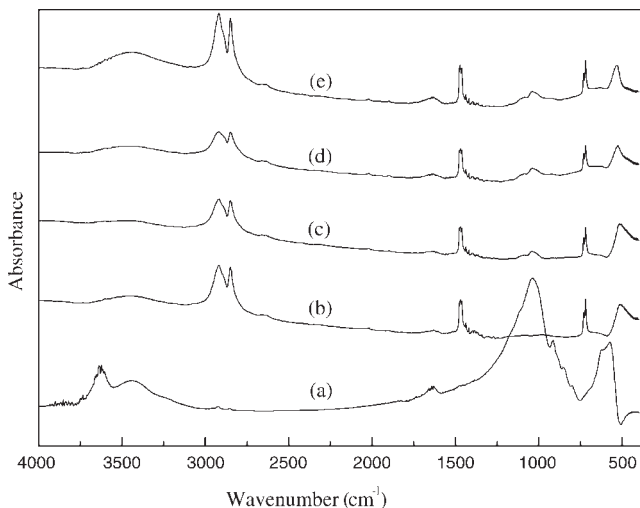


**Figure 2.**

FT-IR spectra of pristine MMT (a), pure PE (b) and the PE/clay nanocomposites (c: PE-1; d: PE-2; e: PE-3).

cates. This confirms that there exist strong interactions between the nanometric silicate layers and the PE segments.

#### Morphology of the PE/Clay Nanocomposites

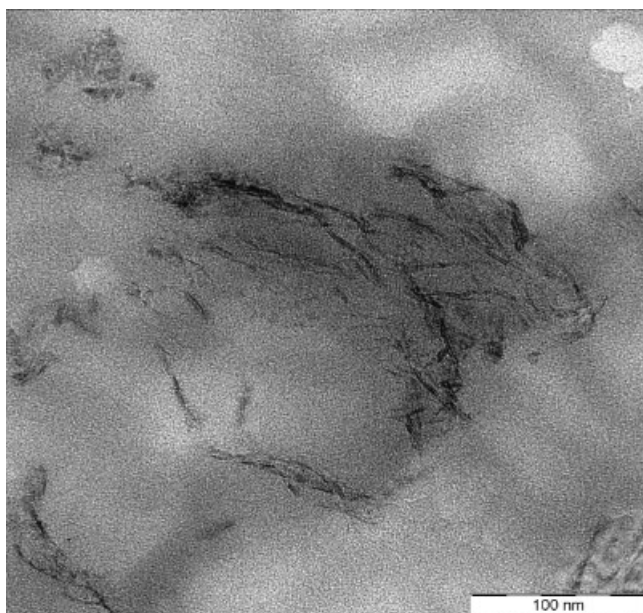
XRD pattern of the PE/clay nanocomposites is shown in Figure 1(c). The  $d_{(001)}$  peak of the clay in the PE nanocomposites completely disappeared. The absence of the (001) peak suggests that the  $d_{(001)}$  spacing between the layered silicates is either intercalated to a spacing greater than the measurable range, or they exfoliate completely in the PE matrix. To further investigate the clay dispersion in polymer matrix, TEM observation was performed.

Figure 3 shows a TEM micrograph of the PE/clay nanocomposite (from sample PE-1) having 3.9 wt % clay. The dark lines represent an individual clay layer and the bright area represents the PE matrix. It can be seen that the aggregated clay particles exfoliate into very thin layers or in stacks of a few layers. The individual silicate layers, along with two or three layer stacks can be observed, and the former are in disordered state and dispersed in the PE matrix. This type of morphology consists of discrete zones of exfoliated particles scattering in

the PE matrix. Thus, it can be concluded that the stacked clay layers exfoliate into nanometer-size layers and disorderly disperse in the PE matrix during the polymerization.

#### Mechanical Properties of PE/Clay Nanocomposites

The effects of the contents of clay on the tensile properties of PE composites are investigated, as shown in Figure 4. The tensile strength and modulus increase with increasing contents of the clay in PE matrix. The tensile strength increases with the content of clay in the PE matrix from 4.0 to 12.9 MPa. The enhancement in strength is directly attributable to the good compatibility between clay and polymer phase and the reinforcement provided by the dispersed silicate nanolayers. Young's modulus of these nanocomposites gradually increase with the clay contents in a range from 22.2 to 37.2 MPa. In the case of nanocomposites, the extent of the improvement of the modulus depends directly upon the average length of the dispersed clay particles, and hence the aspect ratio. As the PE/layered silicate interaction is improved, the stress is much more efficiently transferred from the polymer matrix to the

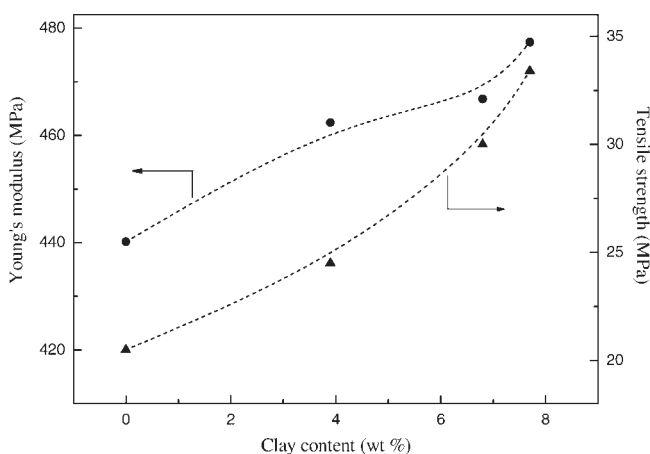


**Figure 3.**  
TEM images of the PE/clay nanocomposites (from sample PE-1).

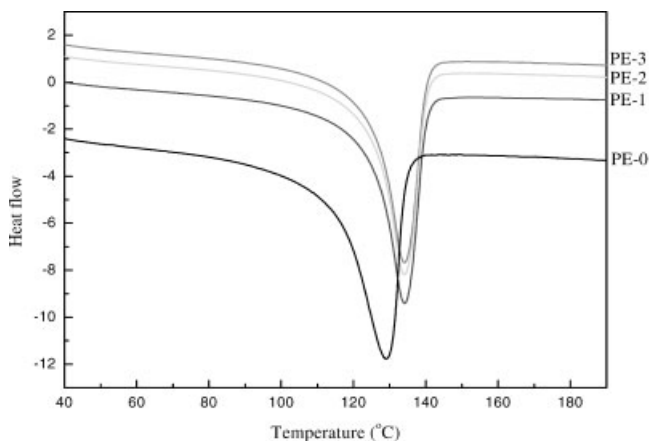
inorganic filler, resulting in a higher increase in tensile properties. These results further confirm the importance of strong interaction between PE matrix and clay, which ultimately leads to better overall dispersion, as already observed by TEM analysis.

#### Thermal Properties of PE/Clay Nanocomposites

DSC curves of pure PE and the PE/clay nanocomposites with different clay contents are shown in Figure 5. The endothermic peak of PE/clay nanocomposites (at around 134.0 °C) appears at obviously



**Figure 4.**  
Effect of the clay content on the tensile properties of the PE/clay nanocomposites.

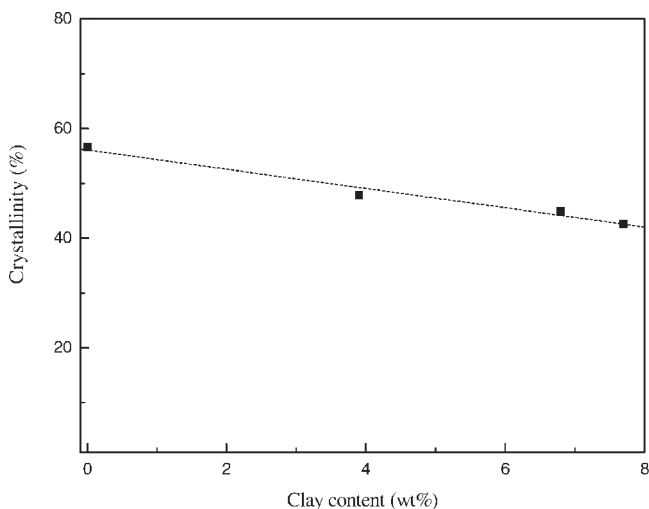
**Figure 5.**

DSC heating thermograms of pure PE and the PE/clay nanocomposites.

higher temperature than that of pure PE (sample PE-0, 128.6 °C); this result is attributed to the strong interaction between the clay and PE matrix. The interaction restricts the motion of the polymer chain, thus a higher melting temperature of the PE/clay nanocomposites is obtained for polymerizations carried out using the intercalation catalyst, at the same polymerization time, temperature and pressure. The crystallinity was measured based on a melting enthalpy of 293 J/g for 100% crystalline PE.<sup>[14]</sup> Compared with pure

PE, the PE/clay nanocomposites have a lower crystallinity (decreased about 15~30%) with the increase of the clay loadings in the PE matrix, as shown in Figure 6. This decline in crystallinity may be attributed to the confinement of the clay layers and the restriction of the PE molecular chains movement.

The thermal stabilities of the PE/clay nanocomposites and pure PE studied by TGA analysis are shown in Figure 7. The temperature for 5% weight loss is defined as the thermal decomposition temperature

**Figure 6.**

Crystallinity of the PE in the PE/clay nanocomposites.



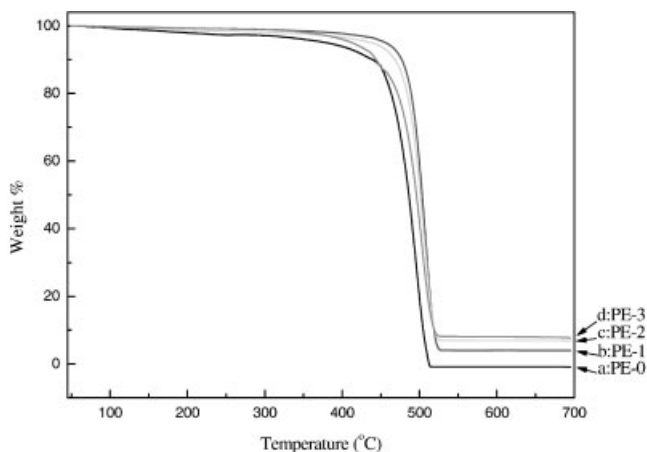


**Figure 7.**

Thermogravimetric analysis of pure PE and the PE/clay nanocomposites.

( $T_d$ ).<sup>[15]</sup> By comparing the curves of PE/clay composites ( $T_{d\text{PE}1\sim3} = 454.6, 436.1, 372.5^\circ\text{C}$ ) with that of PE-0 ( $T_d = 339.8^\circ\text{C}$ ) it can be deduced that the clay layers play an important role in improvement of the thermal stability of the nanocomposites. The good barrier action of the clay layers will help to enhance the thermal stability of the nanocomposites.<sup>[16]</sup> However, the thermal decomposition temperature of the nanocomposites shifts to lower temperature with increasing clay contents. The reason is that the clay itself can also catalyze the degradation of polymer matrixes.<sup>[17]</sup> This action will reduce the thermal stability of the PE/clay nanocomposites with increasing the clay contents in the PE matrix.

The clay has two opposite functions in the thermal stability of the PE/clay nanocomposite.<sup>[18]</sup> When a low fraction is added into the polymer matrix, the barrier effect of the clay is predominant and thermal stability ( $T_d$ ) increases; further increasing the clay loading, the catalyzing effect will grow to dominant, and the thermal stability of the nanocomposites decreases.

## Conclusion

PE/clay nanocomposites have successfully been prepared by performing *in situ* poly-

merization of ethylene using the Ti-MMT activated by  $\text{Al}(i\text{-Bu})_3$ . The occurrence of the exfoliation of clay layers is confirmed and strong interactions exist between the nanometric silicate layers and polymer segments. The physical and mechanical properties of the PE/clay nanocomposites have been improved noticeably due to exfoliated clay disorderedly dispersed in the PE matrix. The melting temperature and thermal decomposition temperature of the nanocomposites increase with respect to the pure PE, whereas the crystallinity and  $T_d$  decrease with clay contents in PE matrix. The change of the thermal stability of the PE/clay nanocomposite is attributed to two opposite functions of the clay.

**Acknowledgements:** This research was funded by the Center for Ultramicrochemical Process Systems (CUPS) sponsored by KOSEF (2006) and Liqiang Cui was supported by the foreign student scholarship program sponsored by Korea Research Foundation. And also, Dr. J-W. Shin was supported by BK-21 program (2007)

- [1] E. P. Giannelis, *Adv. Mater.* **1996**, 8, 29.
- [2] Z. T. Wang, J. Pinnavaia, *Chem. Mater.* **1998**, 10, 3769.
- [3] R. K. Bharadwaj, *Macromolecules* **2001**, 34, 9189.
- [4] S. S. Ray, M. Okamoto, *Prog. Polym. Sci.* **2003**, 28, 1539.
- [5] [5a] Y. S. Ko, T. K. Han, J. W. Park, S. I. Woo, *Macromol. Rapid Commun.* **1996**, 17, 749; [5b] J. Tudor, D. O'Hare, *Chem. Commun.* **1997**, 603; [5c] J. Heine-



- mann, P. Reichert, R. Thomann, R. Mulhaupt, *Macromol. Rapid Commun.* **1999**, 20, 423; [5d] M. Alexandre, P. Dubois, R. Jerome, G. M. Miguel, T. Sun, J. M. Garces, D. M. Millar, A. Kuperman, WO Patent 9947598, Polyolefin Nanocomposites, US, **1999**.
- [6] [6a] H. G. Jeon, H. T. Jung, S. W. Lee, S. D. Hudson, *Polym. Bull.* **1998**, 41, 107; [6b] K. H. Wang, C. M. Koo, I. J. Chung, *J. Appl. Polym. Sci.* **2003**, 89, 2131; [6c] M. Zanetti, P. Bracco, L. Costa, *Polym. Degrad. Stabil.* **2004**, 85, 657; [6d] M. A. Osman, J. E. P. Rupp, *Macromol. Rapid Commun.* **2005**, 26, 880; [6e] S. Tzavalas, K. Macchiarella, V. G. Gregoriou, *J. Polym. Sci., Part B: Polym. Phys.* **2006**, 44, 914; [6f] R. K. Shah, D. R. Paul, *Polymer* **2006**, 47, 4075; [6g] R. W. Truss, T. K. Yeow, *J. Appl. Polym. Sci.* **2006**, 100, 3044; [6h] Y. H. Lee, K. H. Wang, C. B. Park, M. Sain, *J. Appl. Polym. Sci.* **2007**, 103, 2129.
- [7] [7a] J. S. Bergman, H. Chen, E. P. Giannelis, M. G. Thomas, G. W. Coates, *Chem. Commun.* **1999**, 2179; [7b] L. M. Wei, T. Tang, B. T. Huang, *J. Polym. Sci., Part A: Polym. Chem.* **2004**, 42, 941; [7c] Q. Wang, Z. Y. Zhou, L. X. Song, H. Xu, L. Wang, *J. Polym. Sci., Part A: Polym. Chem.* **2004**, 42, 38; [7d] D. W. Jeong, D. S. Hong, H. Y. Cho, S. I. Woo, *J. Mol. Catal. A: Chem.* **2003**, 206, 205; [7e] T. Sun, J. M. Garces, *Adv. Mater.* **2002**, 14, 128; [7f] J. T. Xu, Q. Wang, Z. Q. Fan, *European Polymer Journal* **2005**, 41, 3011; [7g] S. Ray, G. Galgall, A. Lele, S. Sivaram, *J. Polym. Sci., Part A: Polym. Chem.* **2005**, 43, 304; [7h] Y. J. Huang, K. F. Yang, J. Y. Dong, *Macromol. Rapid Commun.* **2006**, 27, 1278; [7i] J. F. Rong, H. Q. Li, Z. H. Jing, X. Y. Hong, M. Sheng, *J. Appl. Polym. Sci.* **2001**, 82, 1829; [7j] F. Yang, X. Q. Zhang, H. C. Zhao, B. Chen, B. T. Huang, Z. L. Feng, *J. Appl. Polym. Sci.* **2003**, 89, 3680; [7k] Y. H. Jin, H. J. Park, S. S. Im, S. Y. Kwak, S. J. Kwak, *Macromol. Rapid Commun.* **2002**, 23, 135.
- [8] C. Ooka, S. Akita, Y. Ohashi, T. Horiuchi, K. Suzuki, S. Komai, H. Yoshida, T. J. Hattori, *Mater. Chem.* **1999**, 9, 2943.
- [9] H. L. Del Castillo, P. Grange, *Appl. Catal. A: Gen.* **1993**, 103, 23.
- [10] R. Swarnakar, K. B. Brandt, R. A. Kydd, *Appl. Catal. A: Gen.* **1996**, 142, 67.
- [11] J. C. W. Chien, *J. Polym. Chem. Ed.* **1990**, 28, 15.
- [12] S.-Y. A. Shin, L. C. Simon, J. B. P. Soares, G. Schlz, *Polymer* **2003**, 44, 5317.
- [13] J. F. Rong, Z. H. Jing, H. Q. Li, M. Sheng, *Macromol. Rapid Commun.* **2001**, 22, 329.
- [14] M. Alexandre, P. Dubois, T. Sun, J. Garces, M. R. Jerome, *Polymer* **2002**, 43, 2123.
- [15] C. G. Zhao, H. L. Qin, F. L. Gong, M. Fen, S. M. Zhang, M. S. Yang, *Polym. Degrad. Stabil.* **2005**, 87, 183.
- [16] J. Wang, Z. Y. Liu, C. Y. Guo, Y. J. Chen, D. Wang, *Macromol. Rapid Commun.* **2001**, 22, 1422.
- [17] H. L. Qin, S. M. Zhang, C. G. Zhao, M. Feng, M. S. Yang, Z. J. Shu, S. S. Yang, *Polym. Degrad. Stabil.* **2004**, 85, 807.
- [18] M. Zanetti, G. Camino, P. Reichert, R. Mulhaupt, *Macromol. Rapid Commun.* **2001**, 22, 176.